

# Exoemission near phase transitions of epitaxial films of manganites with colossal magnetic resistance

I. V. Krylova

Department of Chemistry, M. V. Lomonosov Moscow State University,  
Leninskie Gory, 119899 Moscow, Russian Federation.  
Fax: +7 (095) 932 8846. E-mail: krylova@kge.msu.ru

Intense exoemission near phase transitions of epitaxial films of the  $\text{La}_{0.16}\text{Sr}_{0.84}\text{MnO}_3$  and  $\text{La}_{0.35}\text{Pr}_{0.35}\text{Sr}_{0.3}\text{MnO}_3$ , manganites, which exhibit the colossal magnetic resistance (CMR), is detected in a wide temperature range from 278 to 623 K including the Curie temperature. The role of the absorbed and lattice oxygen in the exoemission and CMR phenomena is discussed. The aftereffect of the magnetic field directed along the film plane on the intensity of photostimulated exoemission is discussed.

**Key words:** exoemission, manganite films, colossal magnetic resistance.

Mixed oxides of the new class,  $\text{Ln}_{1-x}\text{M}_x\text{MnO}_3$  manganites with the perovskite structure containing rare-earth metal ions, exhibit a colossal magnetoresistance (CMR)<sup>1,2</sup> and a strong change in the electroresistance of materials in the presence of magnetic field. This effect is quantitatively characterized by the ratio  $MR = [R(H=0) - R(H)]/R(H=0)$ , where  $R(H=0)$  is the resistance measured in the absence of the magnetic field, and  $R(H)$  is the resistance measured in the field with the  $H$  strength. The CMR is related to a partial substitution of the trivalent ion of a rare-earth element (La, Pr, Nd) by the bivalent cation of an alkali-earth metal (Ca, Sr, Ba), which results in a change in the  $\text{Mn}^{3+}/\text{Mn}^{4+}$  ratio. Electroconductivity and magnetic properties of compounds with CMR are very sensitive to stoichiometry with respect to oxygen atoms and the amount of introduced alkali-earth metal ions.

The CMR phenomena are explained within the framework of the theories of indirect exchange interaction and double Zener exchange<sup>3</sup> in combination with the Jahn-Teller model of structural instability.<sup>2</sup> It is assumed that the same group of electrons is responsible for the magnetic and electric properties of manganites. The manganites with CMR are of great interest due to prospects of their practical application in magnetic recording, as magnetic field sensors, and in other electric and magnetic devices operating in weak magnetic fields as well.<sup>4</sup> The value of  $MR > 10^6$  was obtained<sup>5</sup> for the  $\text{La}_{0.5}\text{Ca}_{0.5}\text{MnO}_3$  antiferromagnetic (AFM).

The first studies of the physical properties of manganites were performed for polycrystalline samples. The next works gave data on CMR of single crystals and thin films. A special attention is given to the magnetic and electron-transport properties of epitaxial films with high resistance. The magnetic and electric properties of polycrystalline samples, single crystals, and epitaxial films grown by the MOCVD (metal-organic chemical vapor

deposition) method have been studied in detail.<sup>6</sup> All samples with the same  $\text{La}_{0.67}\text{Ca}_{0.33}\text{MnO}_3$  and  $\text{La}_{0.67}\text{Sr}_{0.33}\text{MnO}_3$  composition manifest close magnetic and electron-transport properties. At the same time, the electrophysical properties of films and bulk materials with the same composition can strongly differ.<sup>7,8</sup>

The  $\text{Ln}_{1-x}\text{M}_x\text{MnO}_3$  manganites exhibit the semiconductor-metal (SC-M) phase transitions of the second order on going from the high-temperature state with activated conductivity to the low-temperature ferromagnetic phase with metal-like conductivity (FM) at the Curie temperature ( $T_c$ ), holes being charge carriers. The metal-insulator electron phase transition of the first order was found in the external magnetic field. For the  $\text{Nd}_{0.5}\text{Sr}_{0.5}\text{MnO}_3$  sample, a distinct hysteresis of electroresistance was observed during increasing and decreasing the magnetic field intensity at a constant temperature.<sup>9</sup>

For this compound, another phase transition at  $T_{co} \approx T_c$  from the FM phase to the charge-ordered AFM state was found. This transition is accompanied by a resistance jump and a change in the lattice parameters of perovskite. The authors of Ref. 10 plotted the conceptual phase diagram in the  $H-T$  coordinates, which indicates the regions of temperatures and magnetic fields where various states of manganites exist: from the charge-ordered FM (AFM) to the charge-ordered state of the paramagnetic (at elevated  $T$  and low  $H$ ).

The nonstationary low-temperature (4–700 K) exoemission of electrons and ions from metals, semiconductors, and dielectrics under various actions possesses a considerable inertia.<sup>11</sup> Subsequent irradiation at wavelengths exceeding the photoeffect boundary or linear heating leads to the photo- or thermostimulated emission (PSE, TSE), which reflects the energy spectrum of charge localization levels on the surface. The most TSE peaks correspond to the temperatures of structural phase transitions (SPT) in the bulk or on the surface of

solids.<sup>11,12</sup> Observation of the emission at phase transitions usually requires photostimulation, hence, heating (or cooling) is performed simultaneously with irradiation (PTSE).<sup>12</sup> A distinct correspondence has been established between the temperatures of SPT, including  $T_c$ , and exoemission peaks<sup>13</sup> in films of the high-temperature Y–Ba–Cu–O superconductors. We develop a general approach to treating the exoemission that accompany the first and second order phase transitions. The approach is based on the mobility of the structure, appearance and cleavage of strained bonds, and formation of new bonds and structural modifications, *i.e.*, relaxation processes related to the liberation of energy consumed to the yield of weakly bound electrons and ions.<sup>14</sup>

Previously<sup>15</sup> we reported a specific correspondence between the temperatures of FM–SC phase transitions ( $T_c = T_p$ , where  $T_p$  is the temperature of the electroresistance maximum) and PTSE maxima of the epitaxial films of the  $\text{La}_{0.16}\text{Sr}_{0.84}\text{MnO}_3/\text{LaAlO}_3$  (LMS/LAO) and  $\text{La}_{0.35}\text{Pr}_{0.35}\text{Sr}_{0.3}\text{MnO}_3/\text{LaAlO}_3$  (LPSM/LAO) manganites with CMR. This work is aimed at detailed studying TSE and PTSE of these films and examining the results in the 278–623 K temperature region, including  $T_c = T_p$  (according to available published data). We also discuss the role of weakly bound and lattice oxygen in the CMR phenomena according to the TSE (PTSE) data and the influence of the residual magnetization on the exoemission intensity from the manganites.

## Experimental

The LMS/LAO and LPSM/LAO films were prepared by the MOCVD method with the Aerosol source of vapor of organometallic compounds on the single crystal [001]  $\text{LaAlO}_3$  plate in a reactor with inductive heating of the substrate.<sup>16</sup> After precipitation, the films were subjected to annealing in oxygen at the deposition temperature (1000 K) for 30 min. This procedure removed residues of organic compounds used in the film synthesis. The sample simultaneously absorbed oxygen, which is adsorbed, in particular, on the surface in various forms and oxidation states. According to the X-ray microanalysis data, the film thickness was 300 nm. The perovskite  $\text{LaAlO}_3$  substrate (with the unit cell parameter  $a = 0.3792$  nm) makes it possible to obtain  $\text{La}_{1-x}\text{Sr}_x\text{MnO}_3$  films with [001] orientation. The epitaxial correspondence of the perovskite film lattices and the substrate for the samples used by us was determined by the  $\phi$ -scan method.<sup>16</sup> To find  $T_c$  and  $T_p$ , the magnetization of the LMS/LAO film was studied using a SKVID magnetometer, and the electroresistance was studied by the four-probe method;  $T_c = T_p = 270$  K<sup>16</sup>.

For the LPSM/LAO sample, we used  $T_c = T_p = 340$  K obtained for the ceramics with the same composition.\*

Exoemission was recorded *in vacuo* at a residual pressure of  $10^{-4}$  Pa in a pulse mode using a VEU-6 secondary-electron amplifier within the 278–623 K temperature range. The scheme

\* The data on  $T_c = T_p = 340$  K for the ceramics were presented by O. Yu. Gorbenko. For the LPSM/LAO film,  $T_c$  was determined<sup>15</sup> by the observation of the ferromagnetic resonance on a Beker spectrometer,  $T_c = 330$  K.

of the setup has previously been described in detail.<sup>14</sup> When the gap between the sample and inlet of the detector was 1.5 cm, the electric field strength was at most  $200 \text{ V cm}^{-1}$ . Negative charges were detected when a positive potential was fed to the detector. The magnetic field applied perpendicularly to the charge trajectory allowed the identification of the electron and ion components of emitted charges. Photostimulation was performed using a DRT-230 mercury-quartz lamp through narrow-band filters under UV radiation with wavelengths  $\lambda = 313$  nm (the PSE threshold of the studied samples) or  $\lambda = 257$  nm.

The starting samples were heated in a linear mode with a rate of  $7 \text{ deg min}^{-1}$  with simultaneous detection of "spontaneous" TSE due to the technology of production. No emission appeared on repeated heating. Then multicycle tests were carried out in the following regime: heating to 623 K, then cooling to 278 K with simultaneous detection of PTSE ( $\lambda = 313$  or 257 nm). During measurements of exoemission at both a constant temperature equal to  $T_c$  and subsequent heating–cooling, the transversal magnetic field was applied ( $H = 70$  Oe), *i.e.*, the field is directed along the film plane. Two series of measurements with two samples from the same batch were performed. The sizes of the samples were  $2.5 \times 3 \times 1$  mm.

## Results and Discussion

**Spontaneous emission of starting samples.** It is known<sup>11,14</sup> that the spontaneous emission from real surfaces of metals, semiconductors, and dielectrics, as well as their oxides, is the thermodesorption of negative ions adsorbed during technological treatment and storage ( $\text{O}_2^-$ ,  $\text{OH}^-$ ,  $\text{CO}_2^-$ , and others). The starting LMS/LAO and LPSM/LAO samples emit mainly the  $\text{O}_2^-$  and  $\text{O}^-$  ions formed from oxygen absorbed during calcination and cooling. Negative ions of adsorbed gases ( $\text{CO}_2^-$ ) and water vapor ( $\text{OH}^-$ ) are also emitted.

On heating of the LMS/LAO film, the peaks of spontaneous emission appear at  $\sim 278$  K, which is close to  $T_c$ , and at 353, 453, and 533–563 K (Fig. 1). No emission appears during cooling. The plot of the emis-

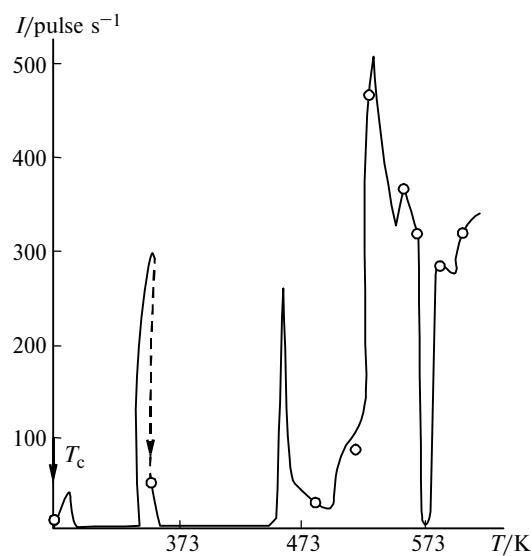
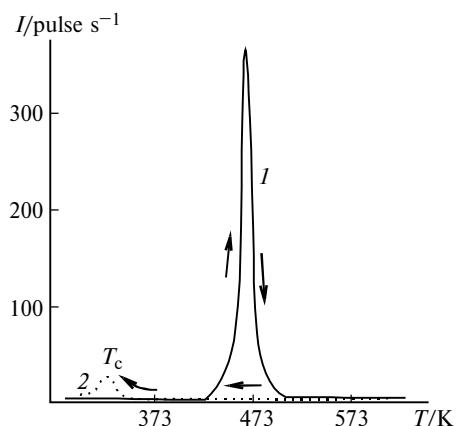


Fig. 1. Spontaneous TSE from the starting LSM/LAO film; M (empty circles) are the points of magnetic field application.



**Fig. 2.** Spontaneous TSE from the starting LPSM/LAO film during heating (1) and cooling (2).

sion intensity vs. temperature for the LPSM/LAO sample contains a sharp maximum at  $T_{\max} = 523$  K. A small splash of the emission current appears during cooling at 343 K, which is close to  $T_c$  (Fig. 2). For the LSM/LAO film (see Fig. 1), the electron and ion components in the negative charge flow were identified. At  $T \leq 373$  K, the magnetic field effect decreased the TSE intensity by ~70%, *i.e.*, negative ions composed 30% charges. At  $T > 473$  K, the magnetic field had no effect on the emission intensity. This implies that only negative ions emitted. TSE did not appear on repeated heating.

Therefore, on the first heating *in vacuo* chemisorbed ions responsible for TSE (including  $\text{CO}_2^-$ ,  $\text{OH}^-$ ) and, perhaps, residues of the starting compounds are removed. The subsequent heating—cooling cycles were carried out under UV irradiation.

**Photothermostimulated emission.** Recording of the spectrum of PSE excitation showed that the photoeffect threshold, under our experimental conditions, lie at  $\lambda = 313$  nm for both samples and the emission increases sharply under UV irradiation ( $\lambda = 257$  nm). Therefore, it seems of interest to consider the absorption spectra of the  $\text{Mn}^{3+}$  and  $\text{Mn}^{4+}$  ions. For  $\text{Mn}^{3+}$ , in addition to the absorption in the visible region ( $\lambda = 500$ – $600$  nm), an intense UV absorption related to charge transfer was found.<sup>17</sup> The  $\text{Mn}^{4+}$  ion absorbs at  $\lambda = 250$  nm and exhibits a sharp growth of absorption at  $\lambda \leq 300$  nm.<sup>17</sup> At the same time, the authors<sup>18</sup> have applied the methods of electron spectroscopy to the high-temperature superconductors (HTSC), cuprates, containing weakly bound oxygen and found that the photoemission occurs due to electrons on the orbitals of the O atoms in the region of bonding energies  $E_b \geq 4$  eV ( $\lambda \leq 313$  nm). An analogy in the behavior of the manganites with CMR and cuprates that possess HTSC has been performed.<sup>2</sup> In both cases, the system gains the metallic properties on doping of the compound with bivalent atoms, which substitute, for example, the La nodes. It has been assumed<sup>2</sup> that in manganites, as in cuprates, the holes are disposed on the oxygen atoms ( $\text{O}^-$ ). However, this was not proved experimentally.

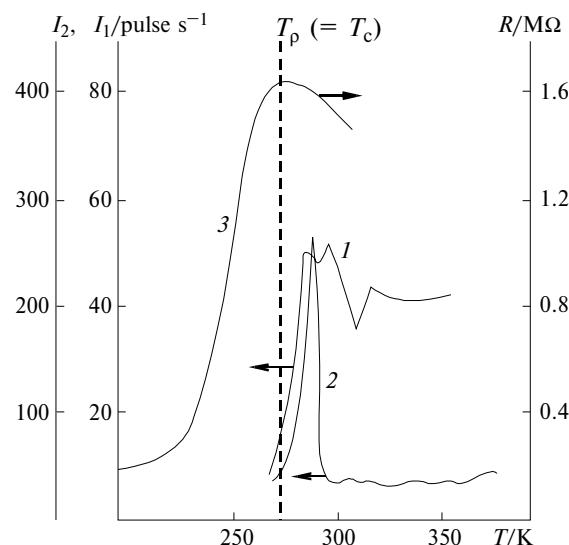


**Fig. 3.** PTSE from the LSM/LAO film in the first ( $\lambda = 313$  nm) (1) and second ( $\lambda = 257$  nm) (2) series of measurements and the temperature plot of the electroresistance<sup>16</sup> (3).

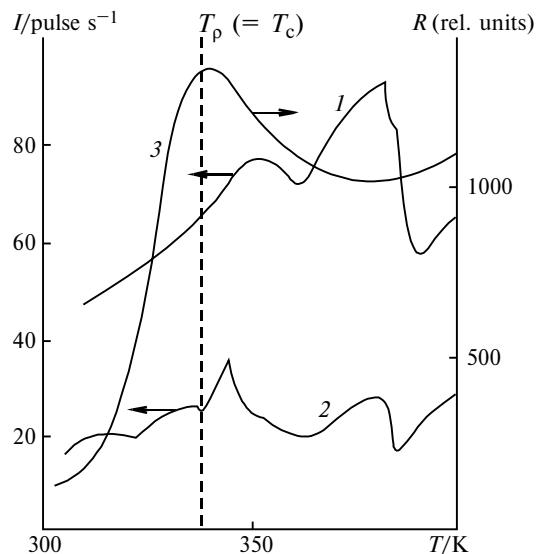


**Fig. 4.** PTSE from the LPSM/LAO film in the first (1) and second (2) series of measurements ( $\lambda = 313$  nm) and the temperature plot of the electroresistance for the ceramics of the same composition<sup>16</sup> (3).

It is seen that splashes of emission currents are observed near  $T_c = T_p$  in the PTSE ( $\lambda = 313$  nm) curves (Figs. 3 and 4) for the LMS/LAO and LPSM/LAO films obtained on the third heating and in the plot of the temperature dependence of the electroresistance.<sup>16</sup> Some shift of the emission peaks toward higher temperatures can be stipulated by different experimental conditions: the resistance was measured in the thermostatted samples in the discrete temperature series, whereas PTSE was detected during the linear heating of the samples.

We found in the first series of measurements that in the fourth heating—cooling cycle the PTSE intensity ( $\lambda = 313$  nm) decreased sharply and was not manifested

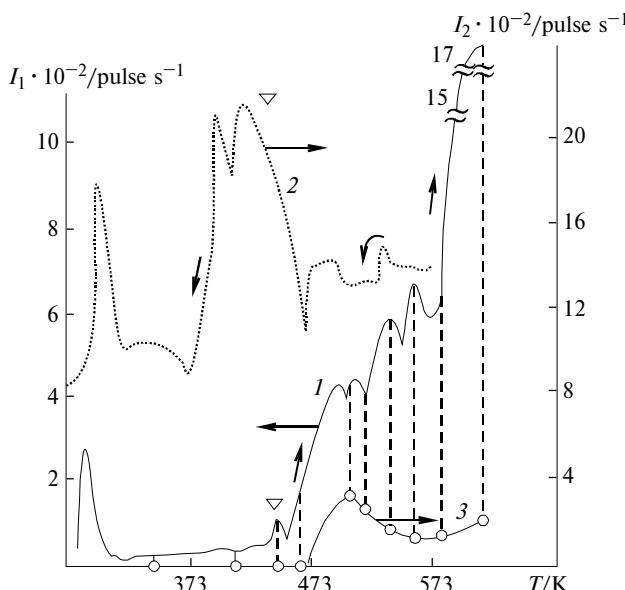
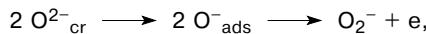


**Fig. 5.** PTSE ( $\lambda = 257$  nm) from the LSM/LAO film on heating (1) and cooling (2) in the third cheating—cooling testing cycle and the ion component of the emission obtained by the magnetic field application (3). The anomalies in the temperature course of the electroresistance<sup>6</sup> ( $\text{La}_{0.67}\text{Sr}_{0.33}\text{MnO}_3/\text{LAO}$  film) are marked (▽); M (empty circles) are the points of magnetic field application.

at all in the fifth cycle. This can be due to the removal by thermovacuum treatment of the weakly bound low-coordinate surface oxygen that forms TSE (PTSE) centers.<sup>11,14</sup> Therefore, in the second series of measurements, the multicycle heating—cooling PTSE tests were performed mainly under UV irradiation ( $\lambda = 257$  nm,  $E = 5$  eV). The results of the second testing series are discussed below.

For the samples of the second series, Figs. 5 and 6 present the more complete PTSE pattern ( $\lambda = 257$  nm) within the 283–623 K temperature interval during the 3rd heating—cooling cycle under the periodical magnetic field effect (M, empty circles). For the LMS/LAO film (see Fig. 5), the peak of the emission intensity near  $T_c = T_p$  is observed during heating and cooling. On cooling from  $T = 573$  to 283 K, the hysteresis (curve 2) takes place, which indicates SPT. Curve 3 obtained during heating in the magnetic field represents the ion component of the emission. The intense emission maximum at  $T = 403$ –423 K during heating (or cooling) is observed for the most studied oxides, including manganites with the spinel structure,<sup>19</sup> and reflects the valent (charge) transformations in the layers of weakly bound oxygen and its desorption (photodesorption)



where  $\text{O}^{2-}_{\text{cr}}$  is the surface low-coordinate ion of the crystalline lattice.<sup>18</sup>

For the LPSM/LAO film (see Fig. 6), the PTSE films in the region of  $T_c = T_p = 343$  K are also observed on both heating and cooling (with some shift over

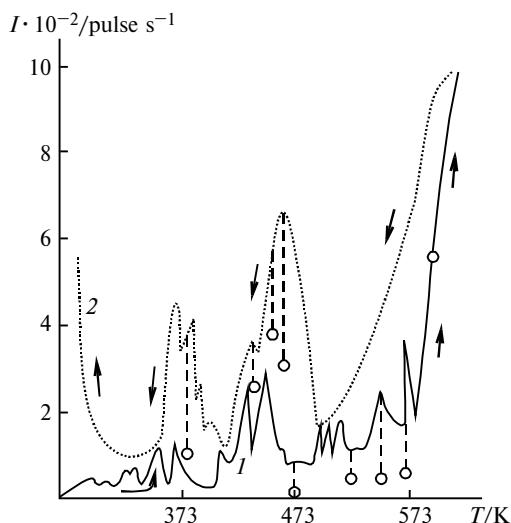


**Fig. 6.** PTSE ( $\lambda = 313$  nm) from the LPSM/LAO film on heating (1) and cooling (2) in the second heating—cooling testing cycle; M (empty circles) are the points of magnetic field application characterizing the ion component of the emission.

temperature). On heating to  $T \approx 573$  K, the PTSE of ions sharply increases monotonically. The peaks at  $T = 423$ –453 K marked above for the LMS/LAO film are also observed. The ion component in the charge flow also appears at  $T > 473$  K. The PTSE hysteresis is especially pronounced at  $T \leq 473$  K, i.e., in the region of SC → FM transition.

Since  $T_c$  and  $T_p$  were measured<sup>16</sup> only in the region below room temperature for the LMS/LAO film and below  $T = 403$  K for the ceramics with the same composition as the LMS/LAO film, the further discussion of the results requires published data. Some increase in the electroresistance, which has not been discussed previously,<sup>16</sup> was detected for the LPSM/LAO sample at  $T > 383$  K (see Fig. 4). For the thin epitaxial  $\text{La}_{0.67}\text{Sr}_{0.33}\text{MnO}_3$  films,  $T_p$  did not coincide<sup>6</sup> with  $T_c$ : a maximum of  $\rho$  was not observed with temperature, as usual, on going to the semiconducting phase, but the electroresistance continuously increased with transition to hopping conduction at  $T_{mi} = 455$  K, which exceeds  $T_c = 360$  K (here  $T_{mi}$  is the temperature of the metal—insulator phase transition). This phenomenon was explained<sup>6</sup> by polaron conductivity: polaron scattering on phonons at  $T > T_c$  gives the positive value  $d\rho/dT$ . The thermally activated hopping conduction by polarons, which is characterized by the negative  $d\rho/dT$  value, occurs above  $T_{mi}$ . This transition (metal—insulator,  $T = 455$  K) appears in the same temperature interval as  $T_{max} = 423$ –453 K in the corresponding PTSE dependence (see Fig. 6) of the manganite films. A transition to the hopping polaron conduction can also be observed in the samples studied by us.

**Thermocyclic tests and SPT.** Thermocyclic tests of the LMS/LAO film were carried out within the 283–623 K temperature range. The fourth heating—cooling testing cycle (PTSE,  $\lambda = 257$  nm) during

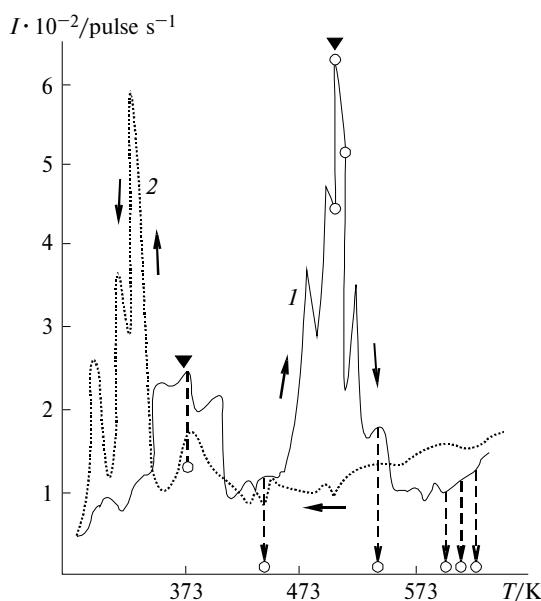


**Fig. 7.** PTSE ( $\lambda = 313$  nm) from the LSM/LAO film on heating (1) and cooling (2) in the fifth testing cycle;  $M$  (empty circles) are the points of magnetic field application, sign  $\blacktriangledown$  designates the temperature of the structural phase transition for the  $\text{La}_{0.85}\text{Sr}_{0.15}\text{MnO}_3$  film (see Ref. 20) or anomalies (the beginning of growth) in the electroresistance at temperatures higher than  $T_c = 204$  K ( $\text{La}_{0.67}\text{Ca}_{0.33}\text{MnO}_3$  film).<sup>5</sup>

heating shows a maximum of the emission intensity in the vicinity of  $T_{\max} = 473$ –503 K. The curve of the PSE intensity on cooling passes below a similar curve obtained on heating of the sample. The pronounced hysteresis with  $T_{\max} = 288$  K appears near  $T_p = T_c$ . The application of the transversal magnetic field showed that electrons are emitted within the whole 288–623 K temperature interval. The main PTSE peak ( $T_{\max} = 493$  K) coincides with the anomalies<sup>5</sup> in the electroresistance curve of the  $\text{La}_{0.67}\text{Ca}_{0.33}\text{MnO}_3$  film. In the fifth testing cycle (Fig. 7), a sharp PTSE peak ( $\lambda = 313$  nm) with  $T_{\max} = 503$  K appears on heating. The ion emission (of oxygen) was found in a narrow temperature region at  $T \approx T_{\max}$ , whereas within the whole remaining temperature interval only electrons were emitted (100%). The PSE hysteresis with a sharp maximum at  $T \approx 330$  K was observed on cooling.

The study<sup>20</sup> of the  $\text{La}_{1-x}\text{Sr}_x\text{MnO}_3$  films with different concentrations of holes ( $x$ ) showed that at  $x = 0.15$ , along with the magnetic phase transition at  $T_c = 250$  K, an anomaly in the run of the electroresistance of the high-temperature magnetic phase ( $T > T_c$ ) is observed, which is due to the structural transition from the rhombohedral to the orthorhombic phase at  $T = 360$  K. This is precisely the temperature at which a broad maximum also attributed to SPT (see Fig. 7) is detected in the PTSE curve on heating of our sample, which is close in composition to the studied one<sup>20</sup> ( $x = 0.16$ ).

In the next sixth and seventh testing cycles, the PTSE intensity ( $\lambda = 313$  nm) decreased dramatically (by

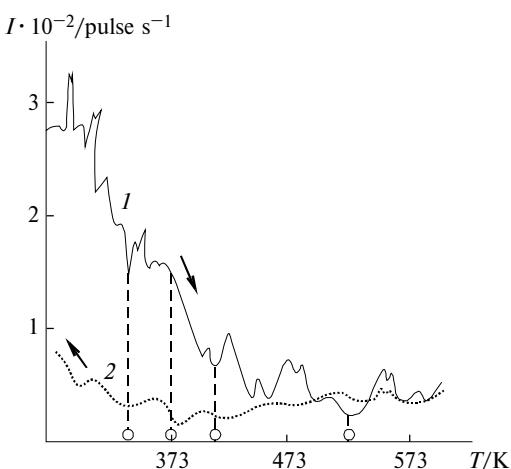


**Fig. 8.** PTSE ( $\lambda = 257$  nm) from the LSM/LAO film on heating (1) and cooling (2) in the eighth testing cycle;  $M$  (empty circles) are the points of magnetic field application.

~5 times) and only electrons were emitted. The PSE hysteresis during cooling was retained, which indicates SPT.

In the eighth testing cycle (Fig. 8), heating of the sample from  $T = 283$  to 623 K results in a monotonic decrease in the PTSE intensity (under UV irradiation at  $\lambda = 257$  nm), and on cooling to  $T_c = T_p = 270$  K the emission increases. Therefore, within the 323–623 K temperature interval the film structure is mainly stabilized.

It has previously<sup>5</sup> been mentioned that the study of the electroresistance at  $T > T_c$  provides a fruitful information about electron transport in the disordered magnetic field. This study was performed<sup>5</sup> for the thin epitaxial  $\text{La}_{0.67}\text{Ca}_{0.33}\text{MnO}_3$  films with CMR obtained by laser sputtering. In these films the magnetoresistance ( $MR$ ) was 14000%. It was found that the activation energy  $E = 0.1$  eV of the resistance  $\rho_0 = f(T)$  remains unchanged to  $T = 503$  K. Within the 503–603 K temperature interval  $\rho_0(T)$  begins to increase slowly with temperature. This phenomenon is explained<sup>5</sup> by the predomination of the electron-phonon interaction over charge transport. Similar results have been obtained<sup>6</sup> for the thin epitaxial films grown by the MOCVD method on the  $\text{La}_{0.67}\text{Sr}_{0.33}\text{MnO}_3/\text{LAO}$ , which did not exhibit activated conductivity up to  $T = 503$  K, exceeding  $T_c = 360$  K. This is related to conduction by heavy carriers (polarons, scattered phonons), which results in the positive value of  $d\rho/dT$ .<sup>6</sup>

A comparison of our data (see Fig. 7) with the previously published<sup>5,6</sup> results indicates the correspondence between  $T_{\max}$  of PTSE and  $T = 503$  K, at which changes in the character of the electroconductivity (the temperature run of the electroresistance) are observed.

It has been established<sup>13,14</sup> that the exoemission intensity increases in the series metal–semiconductor–insulator where the emission occurs from the localized states. The positions of the emission peaks coincide

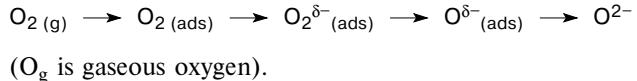
with the SPT temperatures. Therefore, we may expect that at  $T = 503$  K these manganites exhibit the structural (and electron) transition resulting in a change in the character of electroconductivity<sup>5,6</sup> and the appearance of an exoemission maximum.

**Role of oxygen in CMR and PTSE phenomena.** The role of absorbed oxygen in the CMR phenomena has been considered in several works.<sup>5,21,22</sup> In particular, two types of the  $\text{La}_{0.67}\text{Ca}_{0.33}\text{MnO}_3$  films annealed at  $T = 1120$  K in oxygen and in argon were studied.<sup>5</sup> The peak in the  $\rho_0(T)$  plot for the samples annealed in an atmosphere of oxygen and argon is observed at  $T_c = 140$  and 204 K, respectively. The sample with a lower  $T_c$  had the maximum  $MR \sim 14000\%$ , and  $MR$  of that with a higher  $T_c$  was 2300%. This agrees with the general tendency for increasing  $MR$  for samples with a low  $T_c$ .

The influence of oxygen on the magnetoresistance in the silicon-supported La—Ca—M—O films obtained by laser sputtering has been studied.<sup>21</sup> The film deposition at high temperatures of the substrate was found to shift the peak in  $\rho = f(T)$  toward low temperatures, and  $\rho$  increases. Stoichiometry with respect to oxygen was analyzed by the EPMA (electron photon mass spectrometry) method. The oxygen content decreases with temperature of the substrate. The main minimum of the EPMA absorption is related to the charge transfer  $2\text{p}(\text{O}) \rightarrow 3\text{d}(\text{Mn})$ . The oxygen content increases on film annealing in oxygen (1 atm) at  $T = 1170$  K. It has been assumed<sup>21</sup> that oxygen stoichiometry in the film is the decisive factor stipulating the ferromagnetic transition of  $T_c$  and the shift of  $T_p$  toward high temperatures. Oxygen determines the oxidized state of the  $\text{Mn}^{3+}-\text{O}-\text{Mn}^{4+}$  ions, which affects the Mn—O bond length and a probability of electron transfer in the double exchange mechanism. No structural phase transformation, which could be attributed to changes in oxygen stoichiometry, was observed. However, metal oxides are often disordered due to an oxygen deficiency, which influences on the mean path length of electrons: the mobility of the carriers decreases and the resistance increases.<sup>21</sup>

A multiple thermovacuum treatment resulting in a partial removal of weakly bound oxygen leads (see Figs. 5–8) to the disappearance of the PTSE peaks, which reflect SPT in the film at  $T_c > 270$  K. A decrease in the intensity and the disappearance of the emission peaks (see Fig. 8) occur after a sharp ejection of oxygen ions (possibly in the form of  $\text{CO}^-$ ) at  $T = 503$  K (see Fig. 7), which was detected by the results of magnetic field effect on the flow of emitted charges.

Various forms of adsorbed oxygen ( $\text{O}_{\text{ads}}$ ) are known<sup>23</sup>:



It has been shown<sup>24</sup> that at  $T < 448$  K oxygen is retained on the oxides in the form of  $\text{O}_2^-$ , and at  $T > 498$  K the  $\text{O}^-$  ions are formed. This is precisely the temperature  $T = 498$  K (see Fig. 7) at which we

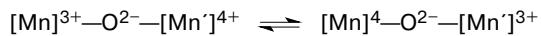
observed a sharp ejection of the ion emission, which is related, most likely, to the photothermodesorption of  $\text{O}^-$ . According to the data of oxygen thermodesorption for some oxides, two peaks have been established<sup>24</sup>: at  $T = 458$  and 558 K. The first peak was attributed to the desorption of  $\text{O}_2^-$ , and the second peak corresponds to  $\text{O}^-$  desorption.

The main PTSE peak (near  $T_c = T_p = 270$  K) remains unchanged during thermocycling (cf. Figs. 3 and 8). We compared the  $T_c$  temperature for the LPSM/LAO film before measurements of exoemission ( $T_c = 340$  K) and after thermocyclic tests and exoemission detection. According to the ESR data,<sup>15</sup>  $T_c$  of the same sample after measurements of exoemission is 330 K, i.e., CMR is retained and  $T_c$  remains virtually unchanged.

The thin La—Ca—Mn—O films are recommended for application<sup>22</sup> as bolometers due to a sharp change in their resistance near  $T_c$ ; the resistance change depends strongly on the oxygen content. The samples, deficient in oxygen and pre-calcined in dioxygen and then annealed *in vacuo* at  $T = 1173$  K, had a higher resistance than the stoichiometric samples. It has been shown<sup>25</sup> for the epitaxial LAO-supported La—Ca—Mn—O films that annealing in oxygen shifts the position of the magnetoresistance maximum toward elevated temperatures (from  $T \sim 100$  K to  $T > 200$  K), resulting in an increase in  $MR$  from 440 to 1400%.

It seems likely that materials with CMR should have a specific stoichiometry with respect to oxygen. The exoemission methods make it possible to distinguish weakly bound oxygen from lattice "bridging" oxygen responsible for double electron exchange in the CMR phenomena. It is known<sup>11,14,15</sup> that the thermovacuum treatment resulting in the removal of weakly bound oxygen decreases the exoemission intensity from oxides, and  $\text{O}_2$  adsorption increases it. However, for the complex oxides with CMR, thermocycling at  $T = 283$ –623 K with simultaneous UV irradiation has almost no effect on the PTSE intensity in the region of temperatures close to  $T_c = 270$  K (cf. Figs. 5 and 8).

As mentioned previously, the mechanism of the CMR phenomenon is the double Zener exchange<sup>3</sup> taking into account the Jahn—Teller structural instability.<sup>2</sup>



The exchange occurs between delocalized 3d-electrons (the  $t_{2g}$  state) of the manganese ions *via* the mobile 3d-electron (the  $e_g$  state). The Jahn—Teller structural instability is due to the lattice deformation (a decrease in symmetry) near the magnetic ions. At the SPT temperature, the lattice deformation results in the formation of strained bonds, "excited states," whose relaxation energy can be consumed to the yield of weakly bound (mobile) electrons (in the  $e_g$  state) beyond the crystal.<sup>13,14</sup> An additional energy ( $E \geq 4$  eV) is provided by the light.

**Magnetic field aftereffects on PSE.** In addition to the aforesaid, we have to consider the aftereffects of the

magnetic field applied perpendicularly to the direction of photoelectron movement, *i.e.*, along the manganite films, on PSE.<sup>15</sup> After the magnetic field ( $H = 70$  Oe) was switched off, PSE from the LSM/LAO film at  $T_c \approx 270$  K was not observed for several min, and then it increased slowly. The observed effects is explained by the residual ferromagnetism and slow reorientation of small domains in the film. The field applied along the film deviates electrons from its trajectory toward the VEU detector. The magnetic field aftereffect on PSE is also retained at temperatures considerably exceeding  $T_c$ . For example, for the LPSM/LAO film ( $T_c = 340$  K) after magnetic field application during PSE measurements at a constant temperature (540 K), the photocurrent was not observed for ~12 min, after which it increased slowly.

The observed influence of magnetic field aftereffects on the photocurrent indicates a correlation between the motion of electrons and the local orientation of spins<sup>5</sup> and retention of the short-range magnetic order in the manganite films upon their heating to temperatures considerably exceeding  $T_c$ . These concepts agree with the views about the internal Weiss molecular field ( $H_E$ ) in ferromagnets related to the exchange interaction:  $H_E = \lambda M$ , where  $\lambda$  is the molecular field constant, and  $M$  is the magnetization. Then the magnetization in the zero external field appears at  $T_c = C\lambda$  ( $C$  is the Curie constant), and this temperature can considerably exceed the real temperature of the magnetic transformation.

Since the exoemission methods are especially sensitive ( $10^{-9}$  of the number of surface atoms), the observed aftereffects of the weak magnetic field (70 Oe) on PSE detect the presence in the system of precisely local magnetic interactions, which are retained upon its heating to  $T > T_c$ . Perhaps, the field-induced changes in the orientation of magnetic spins<sup>25</sup> have sufficiently long relaxation times. Local electric fields appeared in the charge-ordered states of manganites at elevated temperatures can also affect the PSE intensity.

Our study showed that in a wide temperature range (283–623 K) including  $T_c = T_p$  the phase transitions in the manganite films with CMR determined from the electroresistance, as well as using the magnetic and other methods, are accompanied by splashes of exoemission currents. Thermocycling in this temperature interval decreases the exoemission intensity at  $T > 373$  K but does not affect the intensity at  $T = 283$  K close to  $T_c$  (for the  $\text{La}_{0.16}\text{Sr}_{0.84}\text{MnO}_3$  film). This indicates that weakly bound oxygen (in the form of  $\text{O}_2^-$ ,  $\text{O}^-$ , and others) was removed, but bridging oxygen responsible for PTSE near  $T_c$  and for the Zener double exchange providing CMR is retained. The  $T_c$  value, which characterizes the ferromagnet–paramagnetic phase transition, remains unchanged.

Note in conclusion that the exoemission methods make it possible to determine the width and structure of the metal–semiconductor (ferromagnet–paramagnetic) phase transition in thin epitaxial manganite films with

CMR. Exoemission is a highly sensitive method for the detailed study of the solid surface structure.

## References

1. C. N. R. Rao and A. K. Cheetham, *Science*, 1996, **272**, 369.
2. L. P. Gor'kov, *Usp. Fiz. Nauk*, 1998, **168**, 665 [Russ. Phys. Rev., 1998, **168** (Engl. Transl.)].
3. C. Zener, *Phys. Rev.*, 1951, **82**, 4403.
4. M. H. Kryder, W. Messner, and L. R. Cartley, *J. Appl. Phys.*, 1996, **79**, 4485.
5. C. L. Canedy, K. B. Ibsen, G. Xiao, J. Z. Sun, A. Gurta, and W. J. Gallagher, *J. Appl. Phys.*, 1996, **79**, 4546.
6. G. J. Snyder, R. Hiskes, S. Dicarolis, M. R. Beasley, and T. H. Geballe, *Phys. Rev. B*, 1996, **53**, 14434.
7. H. Y. Hwang, S. W. Cheong, P. G. Radaelli, M. Marerio, and B. Batlogg, *Phys. Rev. Lett.*, 1995, **75**, 914.
8. K. Li, L. Lin, J. Sun, X. J. Xu, J. Fang, X. W. Cao, J. S. Zhu, and Y. H. Zhang, *J. Phys. D*, 1996, **29**, 14.
9. M. Kuwahara, Y. Tomioka, A. Assamitsu, Y. Morimoto, and Y. Tokura, *Science*, 1995, **270**, 961.
10. O. Yu. Gorbenko, A. R. Kaul, N. A. Babushkina, and L. M. Belova, *J. Mater. Chem.*, 1997, **7**, 747.
11. I. V. Krylova, *Usp. Khim.*, 1976, **55**, 2138 [Russ. Chem. Rev., 1976, **55** (Engl. Transl.)].
12. T. Gorecki, *Revista Latinoame de Metallurgia, J. Mater.*, 1987, **7**, 3.
13. I. V. Krylova, O. Yu. Gorbenko, and A. R. Kaul', *Izv. Akad. Nauk, Neorgan. Materialy*, 1997, **33**, 475 [Inorg. Mater., 1997, **33** (Engl. Transl.)].
14. I. V. Krylova, *Khimicheskaya elektronika [Chemical Electronics]*, Izd-vo MGU, Moscow, 1993, 160 pp. (in Russian).
15. I. V. Krylova, O. Yu. Gorbenko, and A. R. Kaul', *Zh. Fiz. Khim.*, 2001, **75**, 707 [Russ. J. Phys. Chem., 2001, **75** (Engl. Transl.)].
16. O. Yu. Gorbenko, R. V. Demin, A. R. Kaul', L. I. Koroleva, and R. Shimchak, *Fiz. Tverdogo Tela*, 1998, **40**, 290 [Sov. Phys. Sol. State], 1998, **40** (Engl. Transl.)].
17. D. T. Sviridov, R. K. Sviridova, and Yu. F. Smirnov, *Opticheskie spektry ionov perekhodnykh metallov v kristalakh [Optical Spectra of Transition Metal Ions in Crystals]*, Nauka, Moscow, 1971, 267 pp. (in Russian).
18. A. A. Lisachenko, Author's Abstract, Doct. Sci. (Phys.-Math.) Thesis, St. Petersburg State Univ., St. Petersburg, 1996, 28 pp. (in Russian).
19. I. V. Krylova, N. M. Panich, and G. N. Pirogova, *Izv. Akad. Nauk, Ser. Khim.*, 1997, 1618 [Russ. Chem. Bull., 1997, **46**, 1543 (Engl. Transl.)].
20. A. Urushibara, Y. Morimoto, T. Arima, A. Asamitsu, G. Kido, and Y. Tokura, *Phys. Rev. B*, 1995, **52**, 1403.
21. W. Zhang, W. Boyd, M. Elliot, and W. Herrenden-Harkerand, *Appl. Phys. Lett.*, 1996, **69**, 3929.
22. J. H. Hao, X. T. Zeng, and H. K. Wong, *J. Appl. Phys.*, 1996, **79**, 1810.
23. C. T. Au, A. F. Carley, A. Pashuski, S. Read, M. W. Roberts, and A. Zeini-Isfahan, in *Adsorption on Ordered Surfaces of Ionic Solids and Thin Films*, Springer, Bad Honnef, 1993, 241.
24. S. R. Morrison, *The Chemical Physics of Surfaces*, Plenum Press, New York–London, 1977.
25. S. Jin, T. H. Tiefel, M. McCormack, R. A. Fastnacht, R. Ramesh, and L. H. Chen, *Science*, 1994, **263**, 413.

Received June 13, 2000;  
in revised form November 1, 2000